INTERNATIONAL ATOMIC ENERGY AGENCY
UNITED NATIONS EDUCATIONAL, SCIENTIFIC AND CULTURAL ORGANIZATION

INTERNATIONAL CENTRE FOR THEORETICAL PHYSICS
34100 TRIESTE (ITALY) - P.O.B. 586 - MIRAMARE - STRADA COSTIERA 11 - TELEPHONE: 2240-1
CABLE: CENTRATOM - TELEX 460392 - I

SMR/390 - 17

WORKING PARTY ON "FRACTURE PHYSICS"
(29 May - 16 June 1989)

MECHANISMS OF STRESS CORROSION CRACKING AND CORROSION FATIGUE

H. VEHOFF
Max-Planck-Institut Für Eisenforschung GmbH
Max-Planck Strasse 1
Dusseldorf 4000
Federal Republic of Germany

MECHANISMS OF STRESS CORROSION CRACKING AND CORROSION FATIGUE

Crack Tip Electrochemistry

Slip Step Dissolution

Grain Boundary Structure
Segregation
Slip Distribution and Localization

Crack Initiation

Strain Localization at Grain Boundaries

Special Bicrystal Orientations

Sensitive for crack initiation in hydrogen
Sensitive for crack initiation by anodic dissolution

Crack Tip Electrochemistry

At a crack tip: potential, pH and composition of the solution is different.

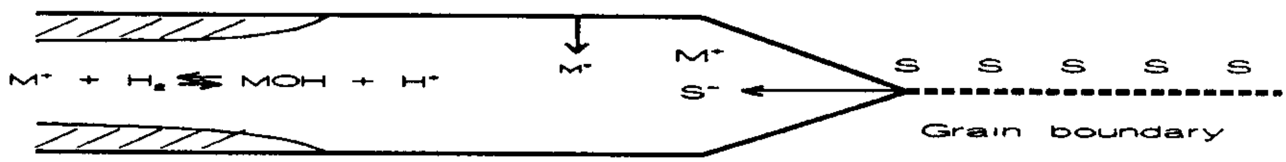

Reactions at crack walls, transport of ions to and from the crack tip change in pH and concentration influence the potential at the electrochemical double layer at the crack tip.

Weeping electrode test

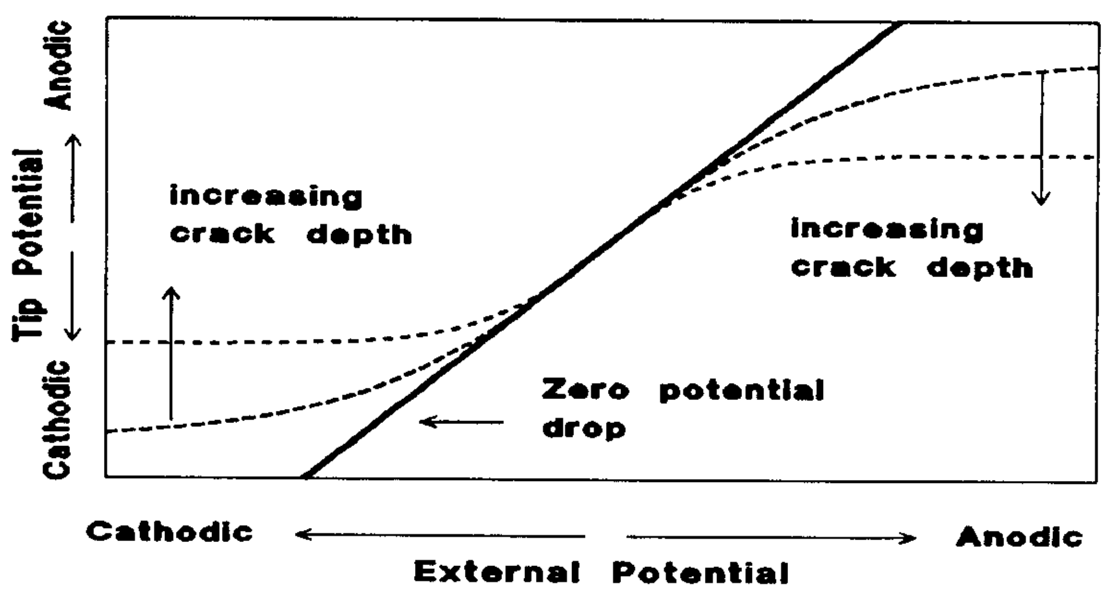

Mass Transport Theory

The flux of dissolved species:

$$j = -M\nabla\mu$$

with $$\bar{\mu} = \mu_0 + RT\ln c + Fze\Phi$$

for each species.

Mass conservation of species

$$\frac{\partial C_i}{\partial t} = -\nabla J_i + R_i$$

R_i represents the rate of production or depletion of a species.
Typical reaction in a crack:

Anodic dissolution

$$M \rightarrow M^{n+} + ne^-$$

hydrolysis reaction

$$M^{n+} + H_2O \leftrightarrow M(OH)^{(n-1)+} + H^+$$

cathodic reduction

$$H^+ + e^- \rightarrow H$$

$$H_2O + e^- \rightarrow H + OH^-$$

where a typical rate equation has the following form

$$R_{H^+} = k_a C(H^+)\exp\left(-\frac{\beta' FE}{RT}\right)$$

and electro-neutrality

$$\Sigma z_i C_i = 0$$

current density

the sensitive potential range for SCC

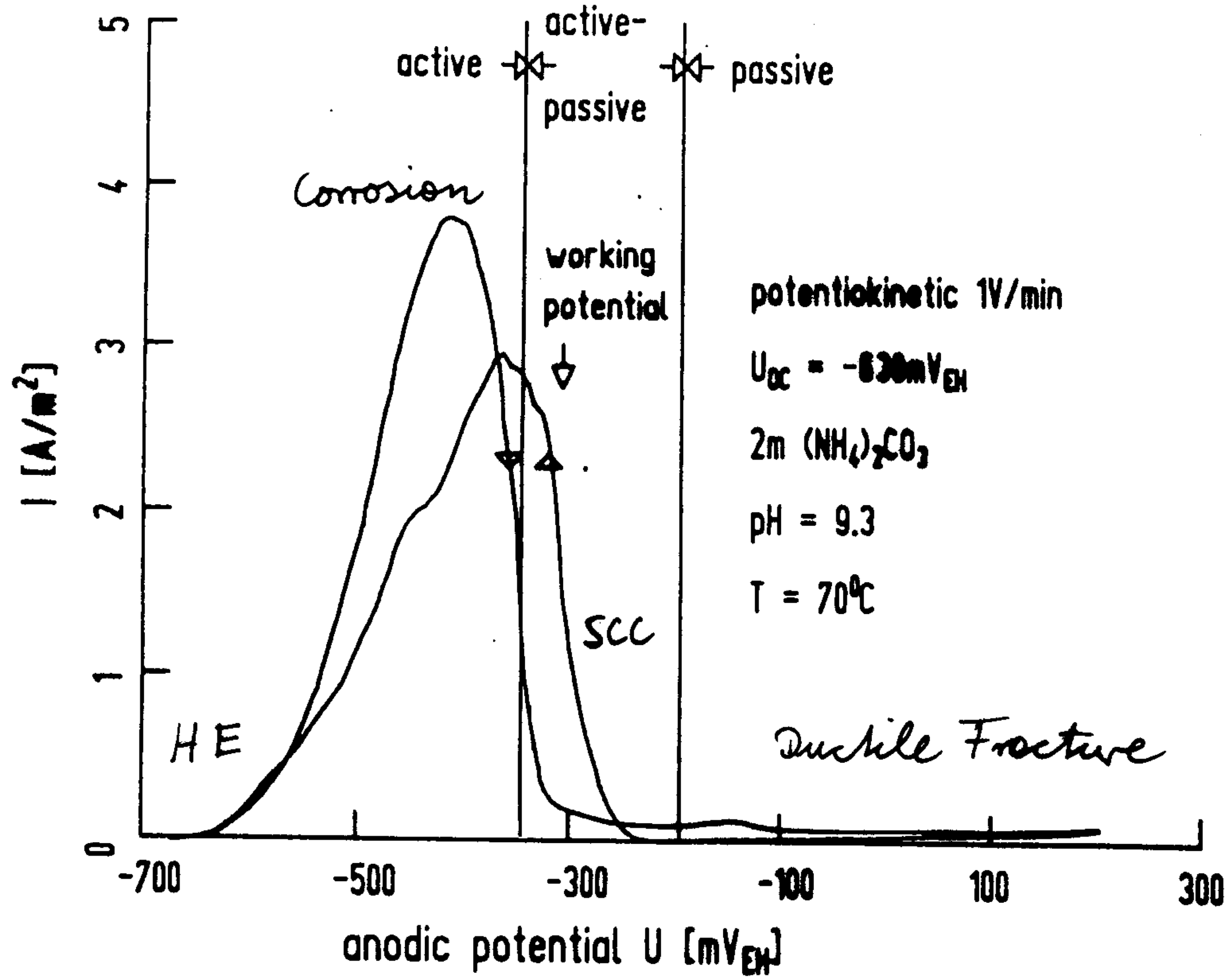

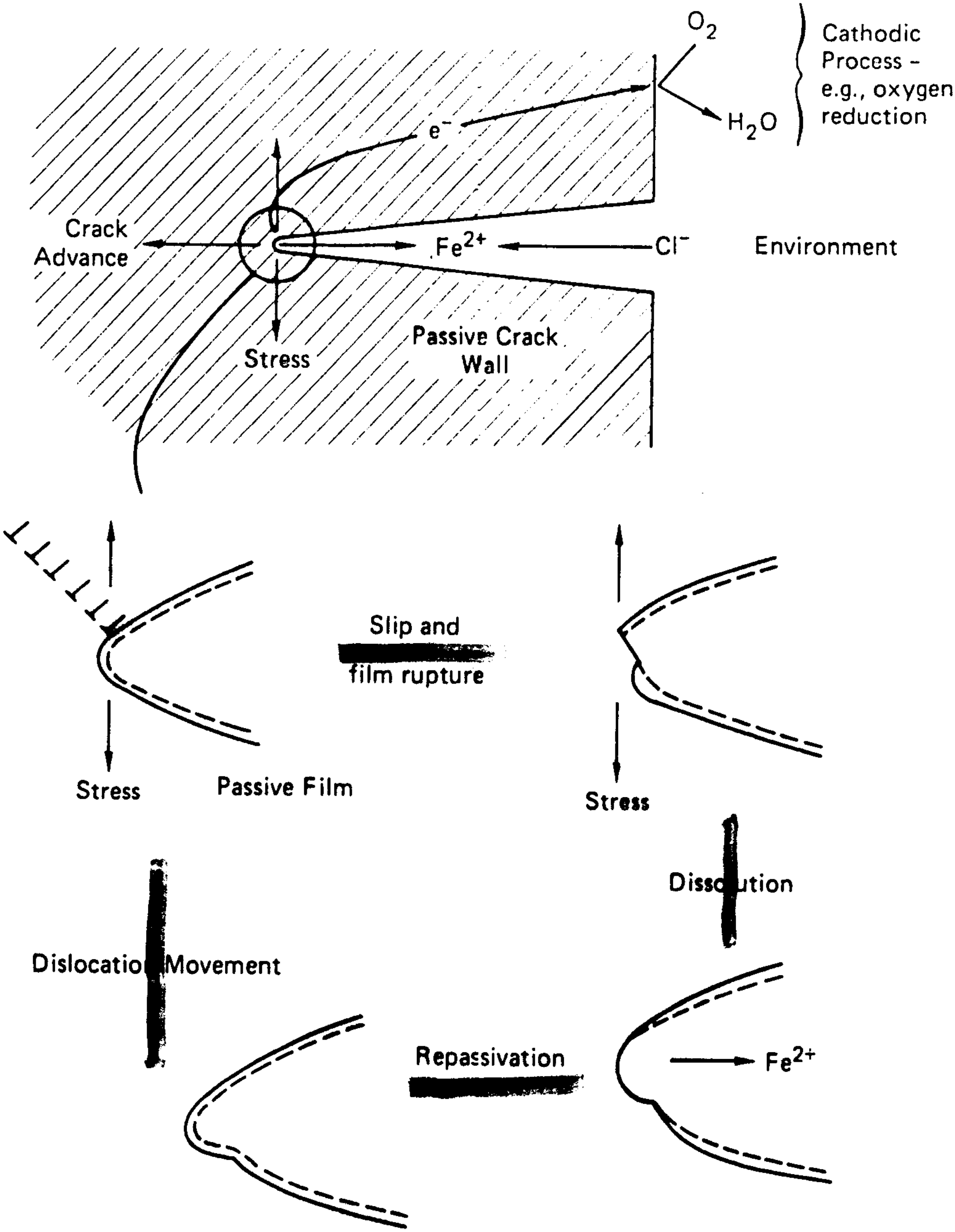
O2
H2O
Cathodic
Process -
e.g., oxygen
reduction
e-
Crack
Advance
Fe2+
Cl-
Environment
Stress
Passive Crack
Wall
Slip and
film rupture
Stress
Passive Film
Stress
Diss ution
Dislocatio Movement
Repassivation
Fe2+

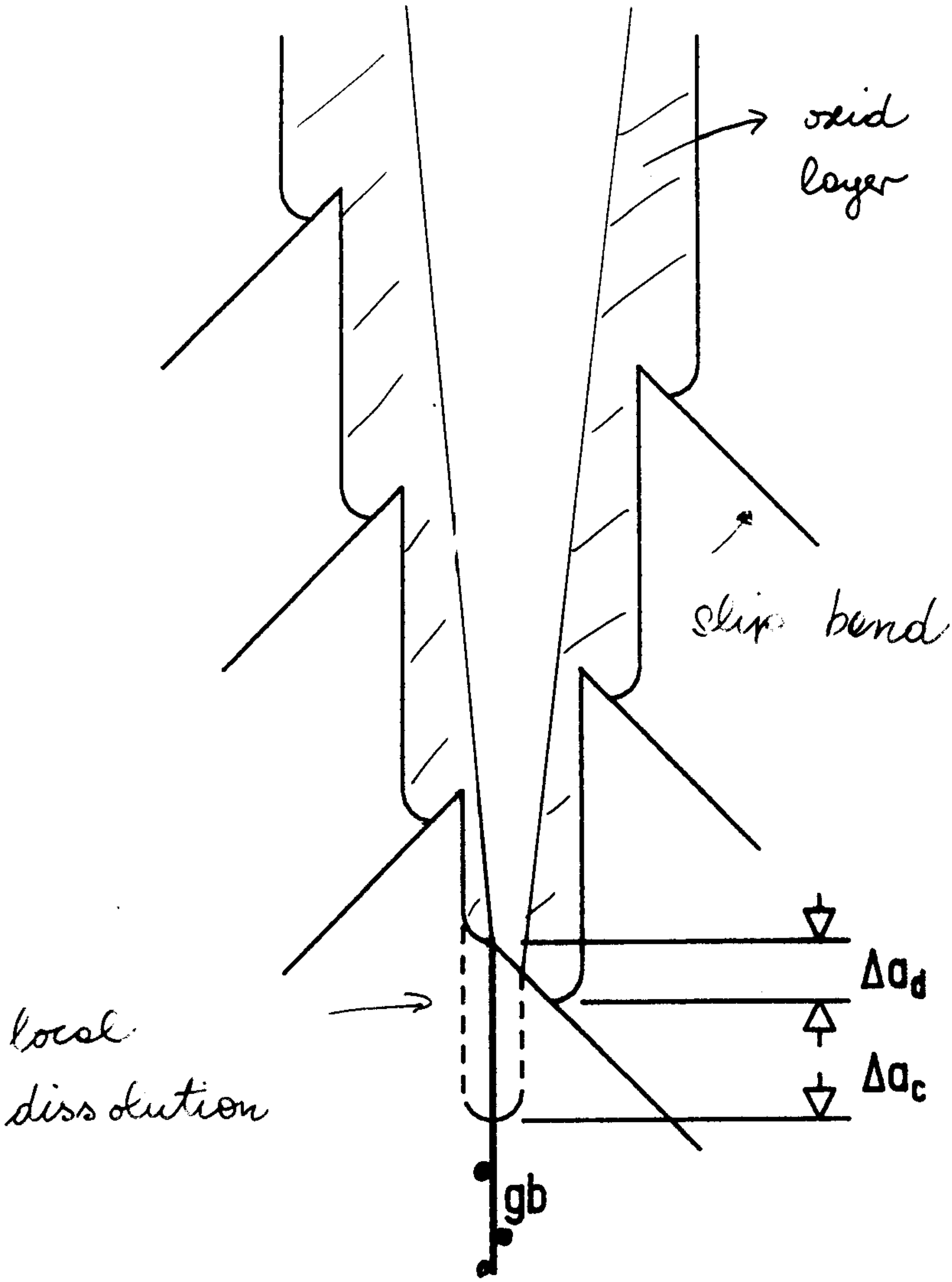

MPI für Eisen-forschung	Reduction of the crack tip angle by slip step dissolution along the grain boundary	Stenzel Vehoff Neumann

Magnification of the crack tip region

$$a_n = \frac{\Delta a_g}{\delta_s}$$

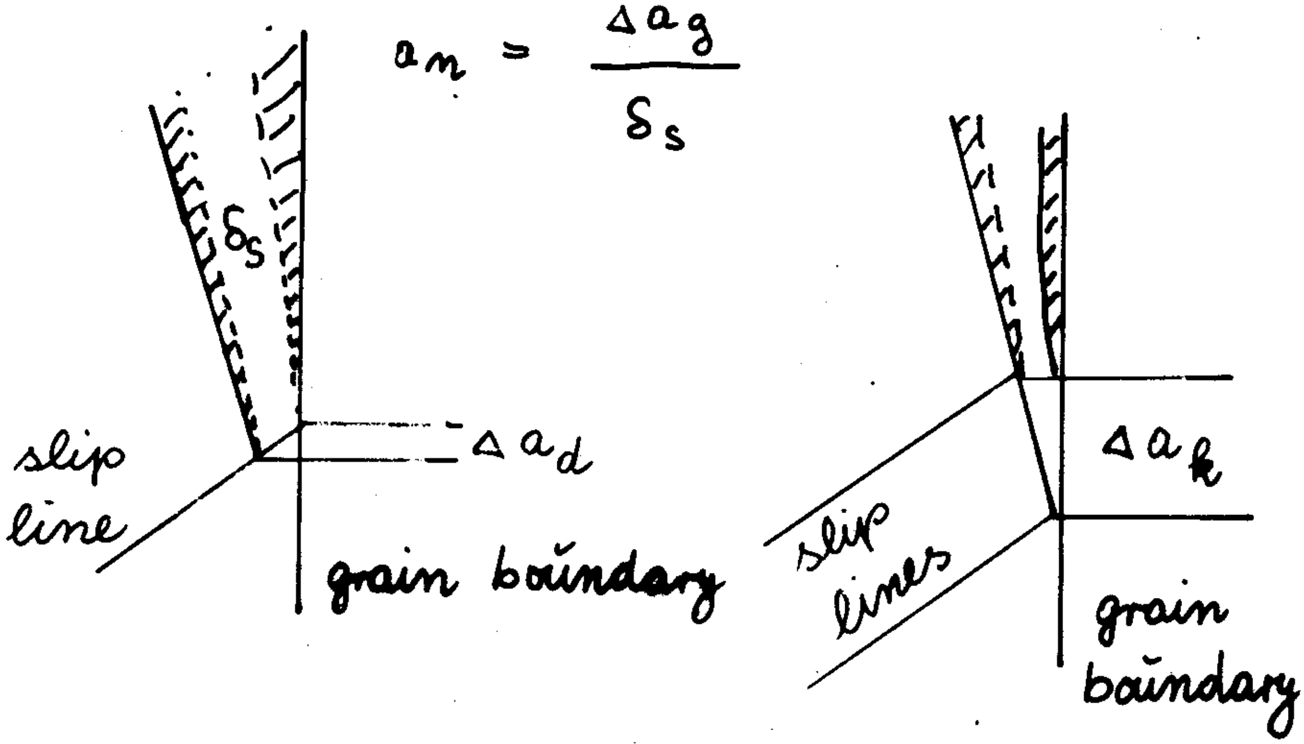

$$\Delta a_g = \Delta a_d + \Delta a_k \ ,$$

$$\Delta a_k = \Delta a_p(1-\exp(-t_s/t_p))$$

t_s = time between slip events
t_p = repassivation time
Δa_p = maximum amount dissolved between two slip events

$$\dot{a} = (a_n/2 + \alpha_1(1-\exp(-\alpha_2/\dot{\delta}))\dot{\delta}$$

δ_s = plastic crack tip opening between two slip events

$\alpha_1 = \Delta a_p/\delta_s$; $\alpha_2 = \delta_s/t_p$

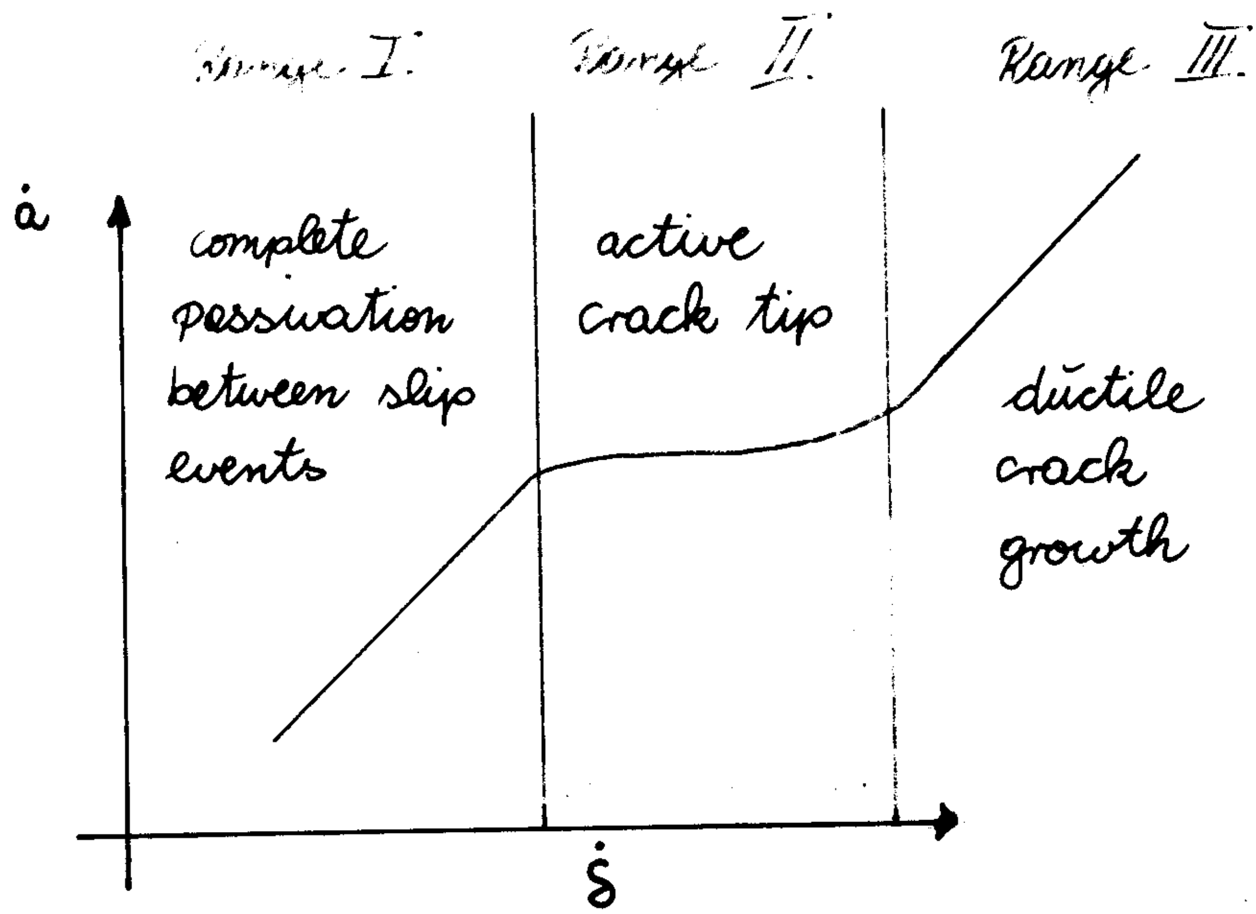

I. [redacted] strain [redacted] and fast passivation

$(t_p << t_s)$

$$\dot{a} = (a_n/2 + \Delta a_p/\delta_s)\dot{\delta}$$

II. [redacted] strain [redacted] and slow passivation

$$\dot{a} = (a_n/2)\dot{\delta} + \Delta a_p/t_p = \dot{a}_d + \dot{a}_c$$

III. [redacted] strain [redacted]

$$\dot{a} = (a_n/2)\dot{\delta}$$

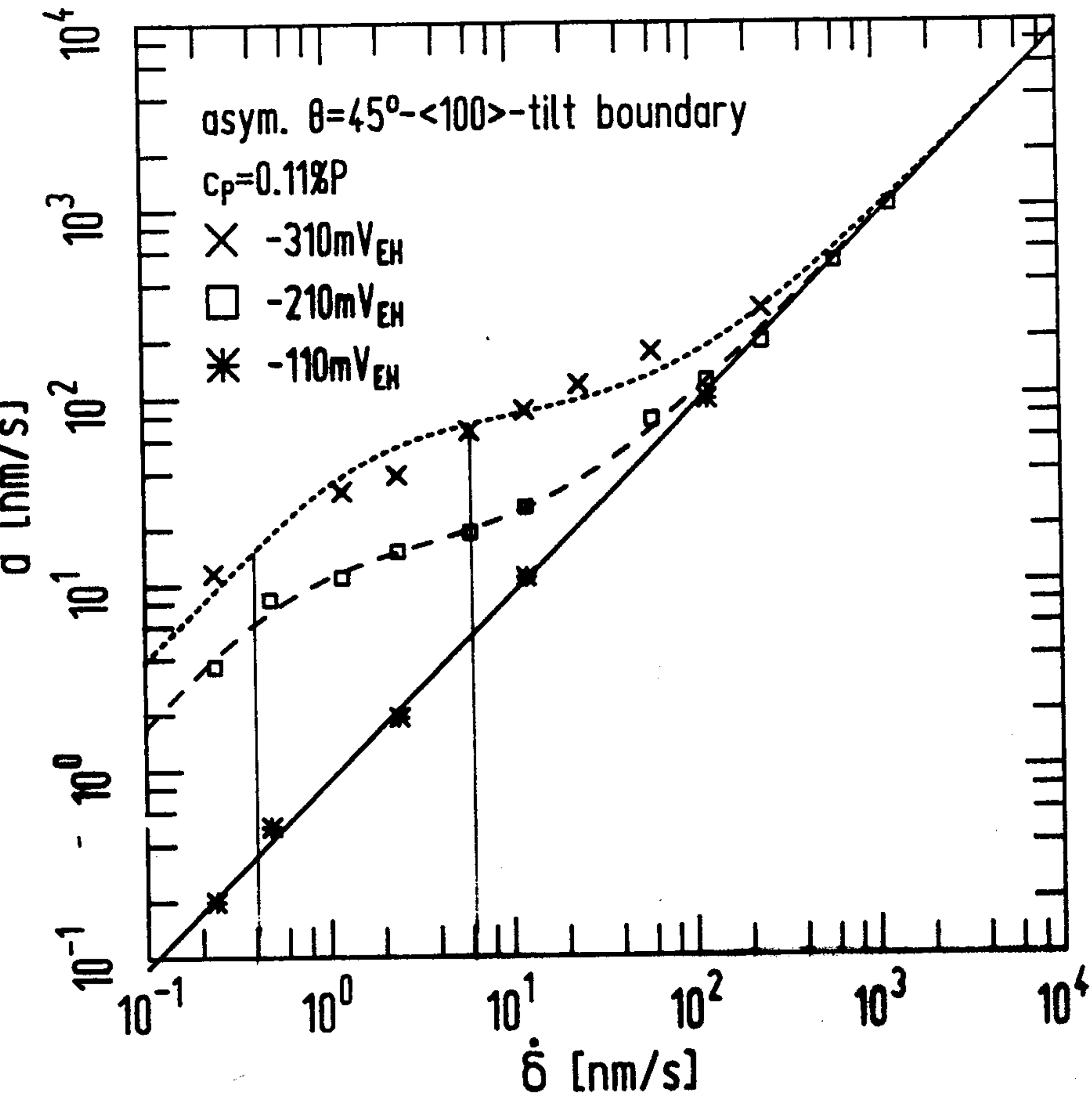

b Influence of Potential on SCC

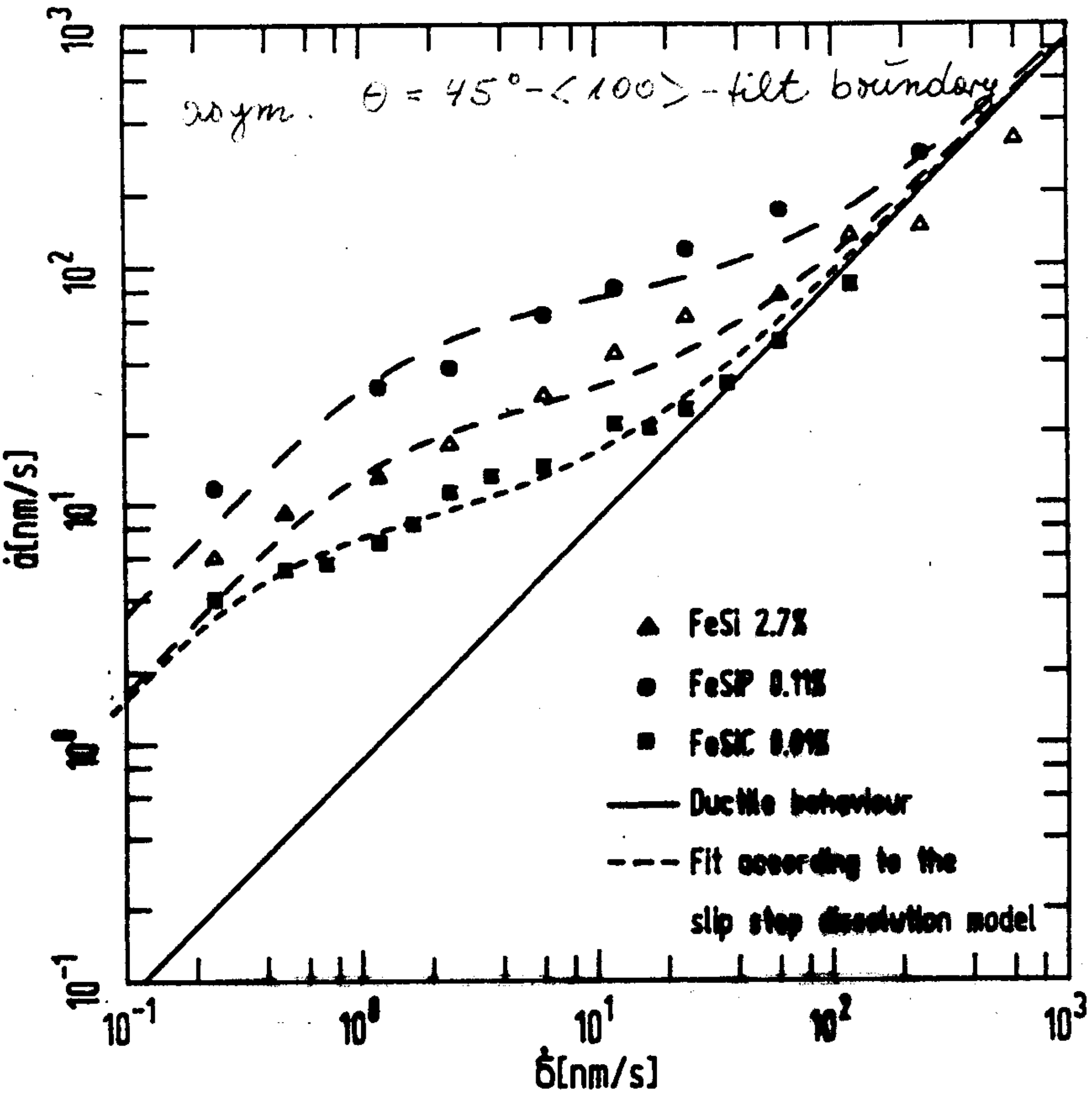

Influence of segregation on SCC

Clean boundaries show SCC in this system.

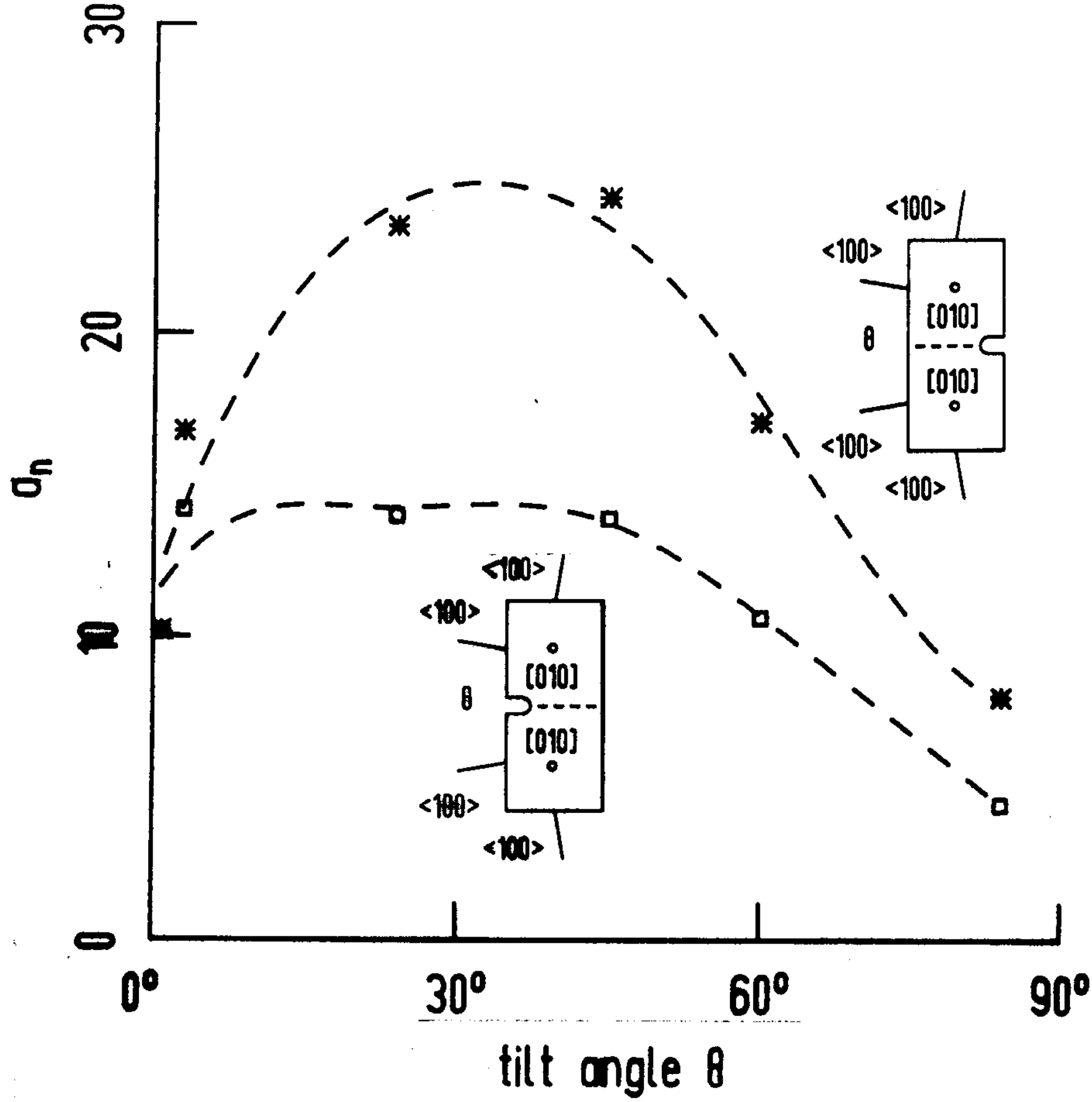

* and □ are measurements for the same boundary, only the slip distribution at the crack tip is different.

→ localisation of slip increases the growth rate of Stress Corrosion Cracks

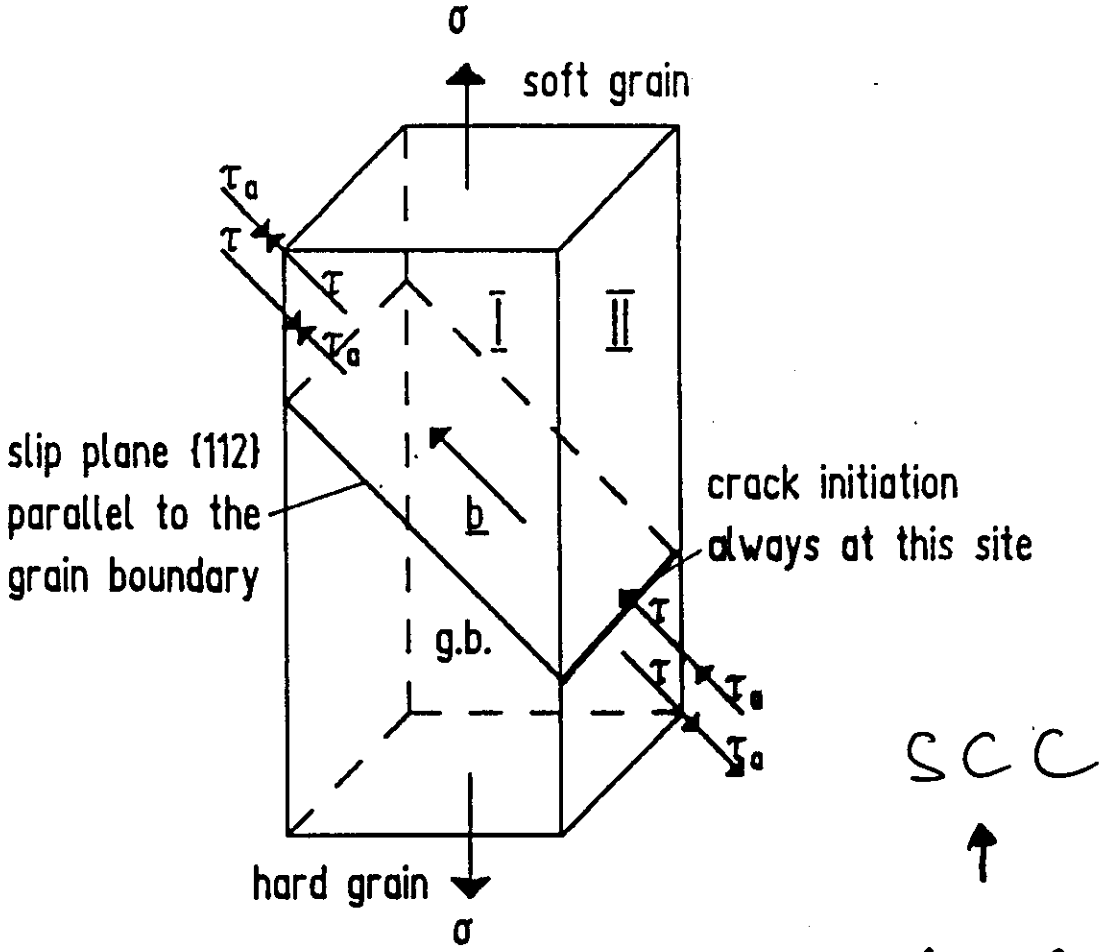

Sensitive orientations for the nucleation of cracks by

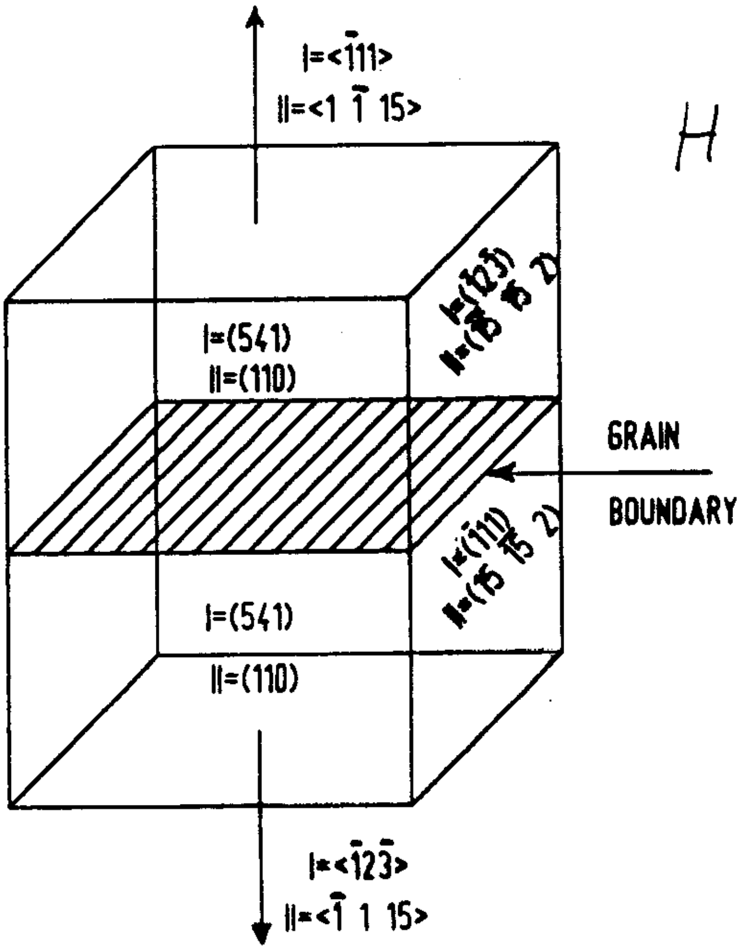

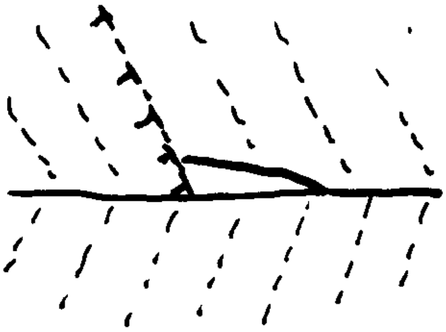

Annealed Austenitic Steel

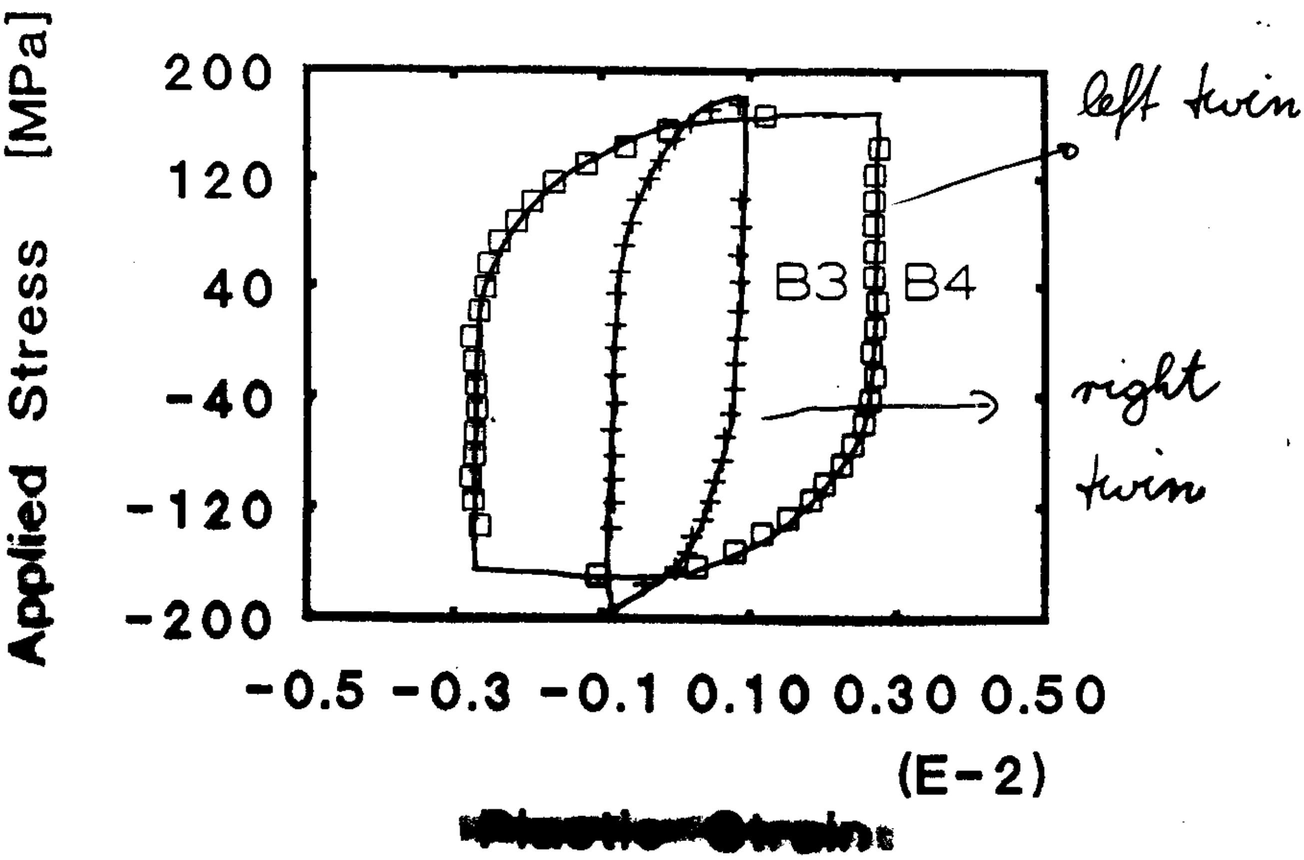

Hein, 1989

Localized Plastic Strain at a Grain Boundary

measured by Laser Interferometrie

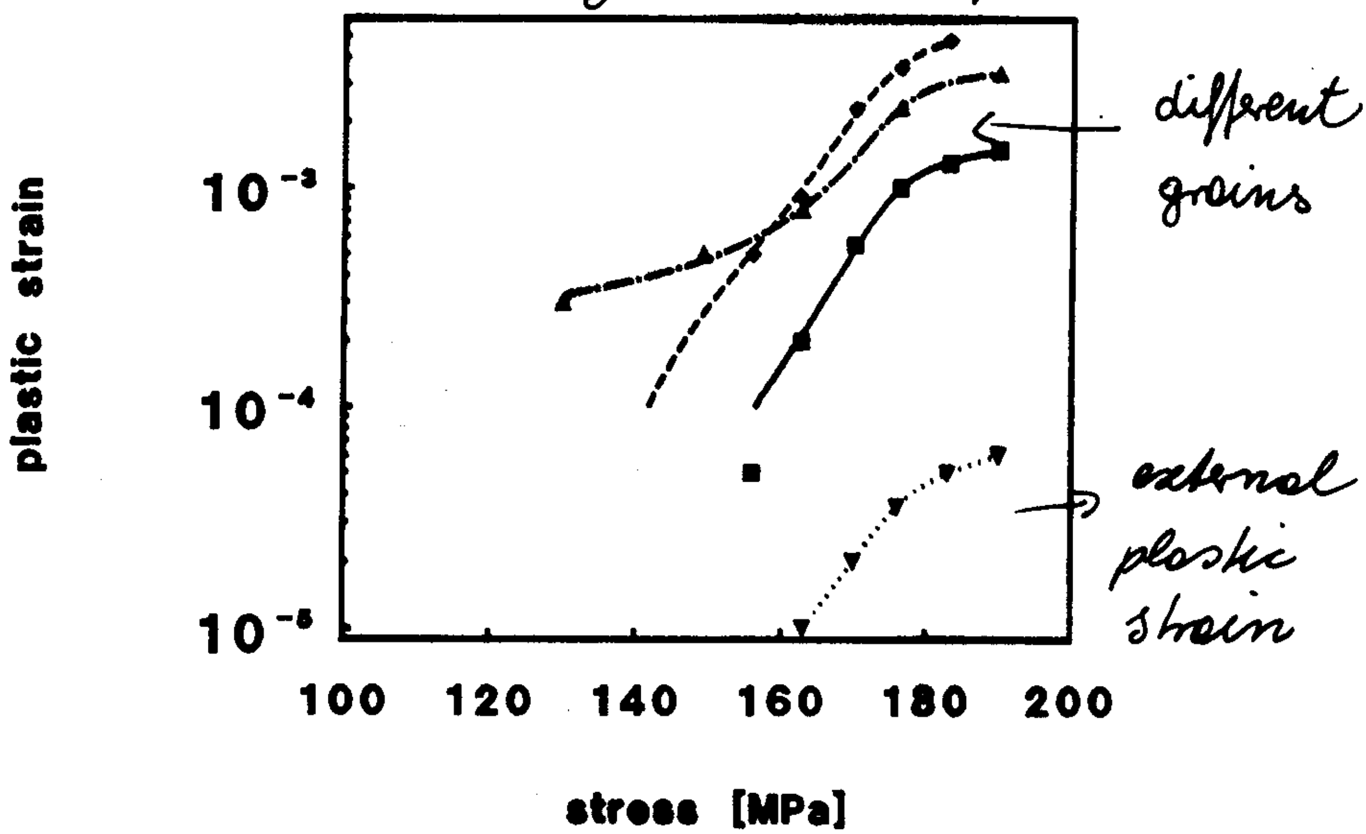

endurance limit is reduced by a factor of two.

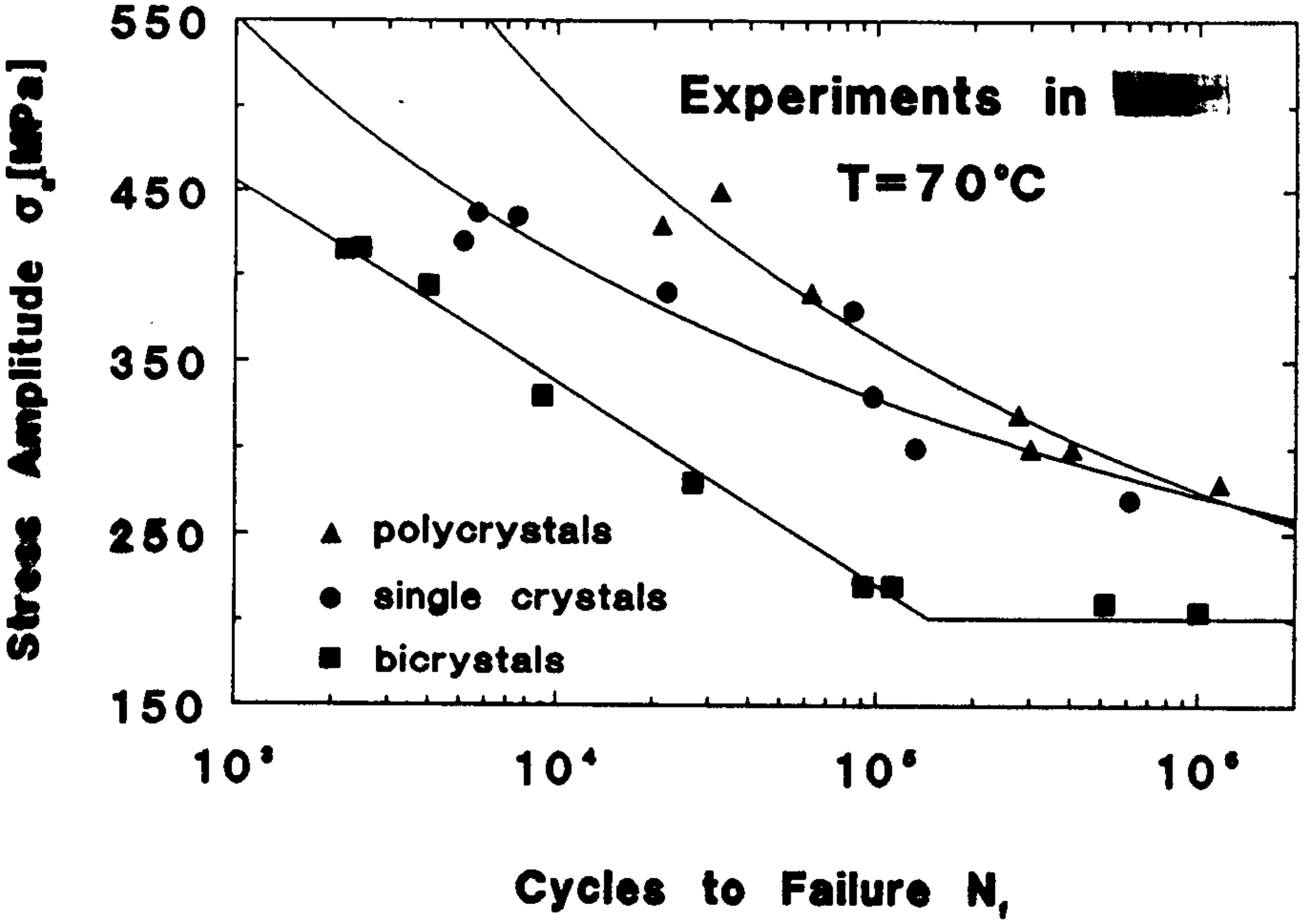

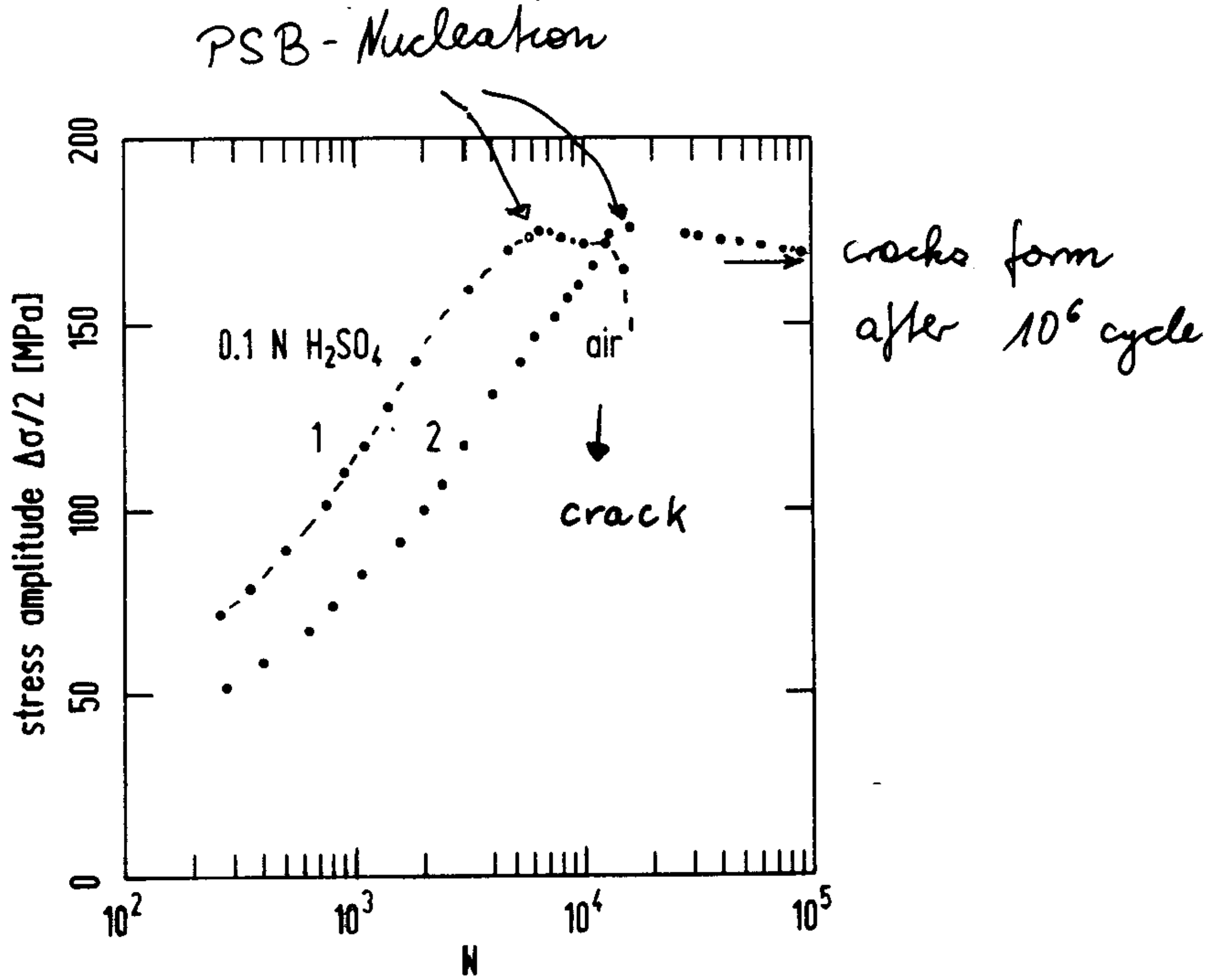
PSB - Nucleation
cracks form after 10⁶ cycle
0.1 N H2SO4
air
crack
1
2
stress amplitude Δσ/2 [MPa]
N

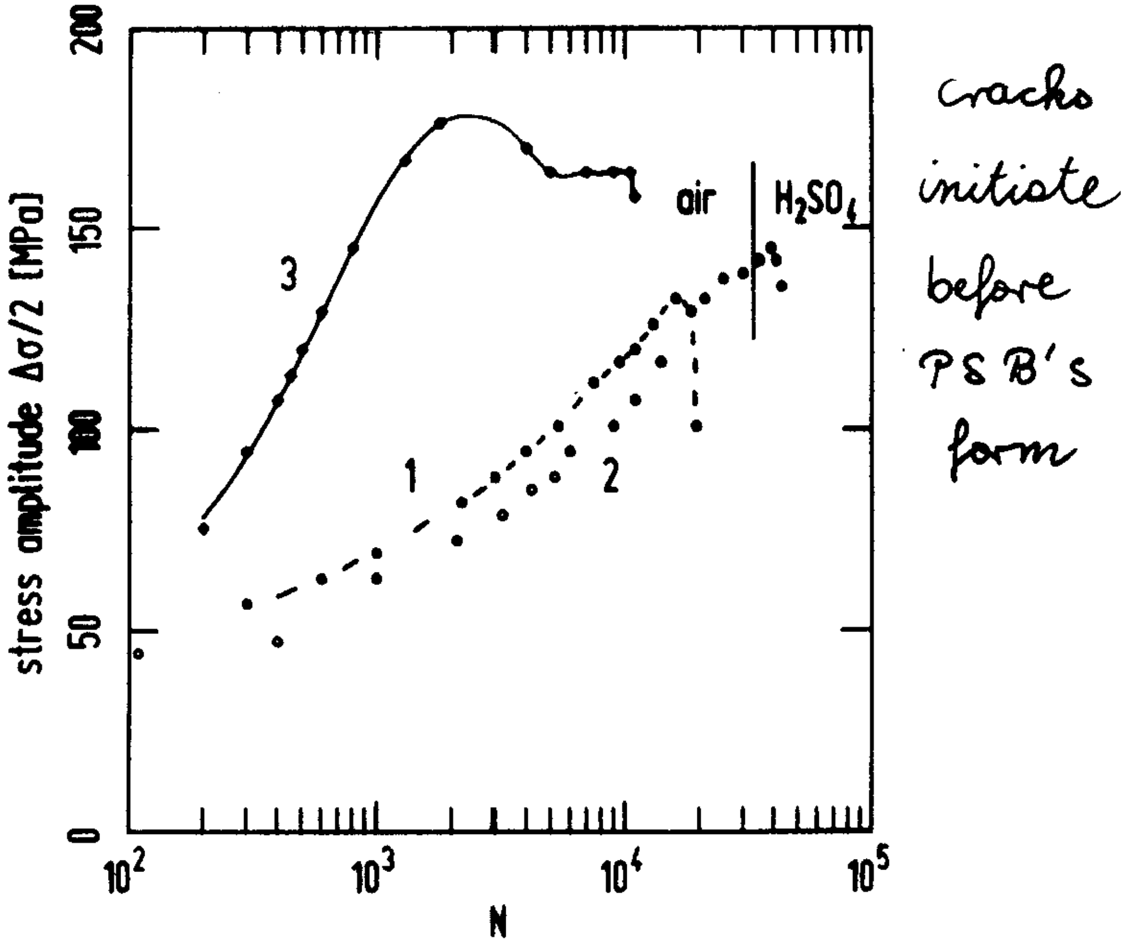
cracks initiate before PSB's form
3
1
2
air
H2SO4
stress amplitude Δσ/2 [MPa]
N

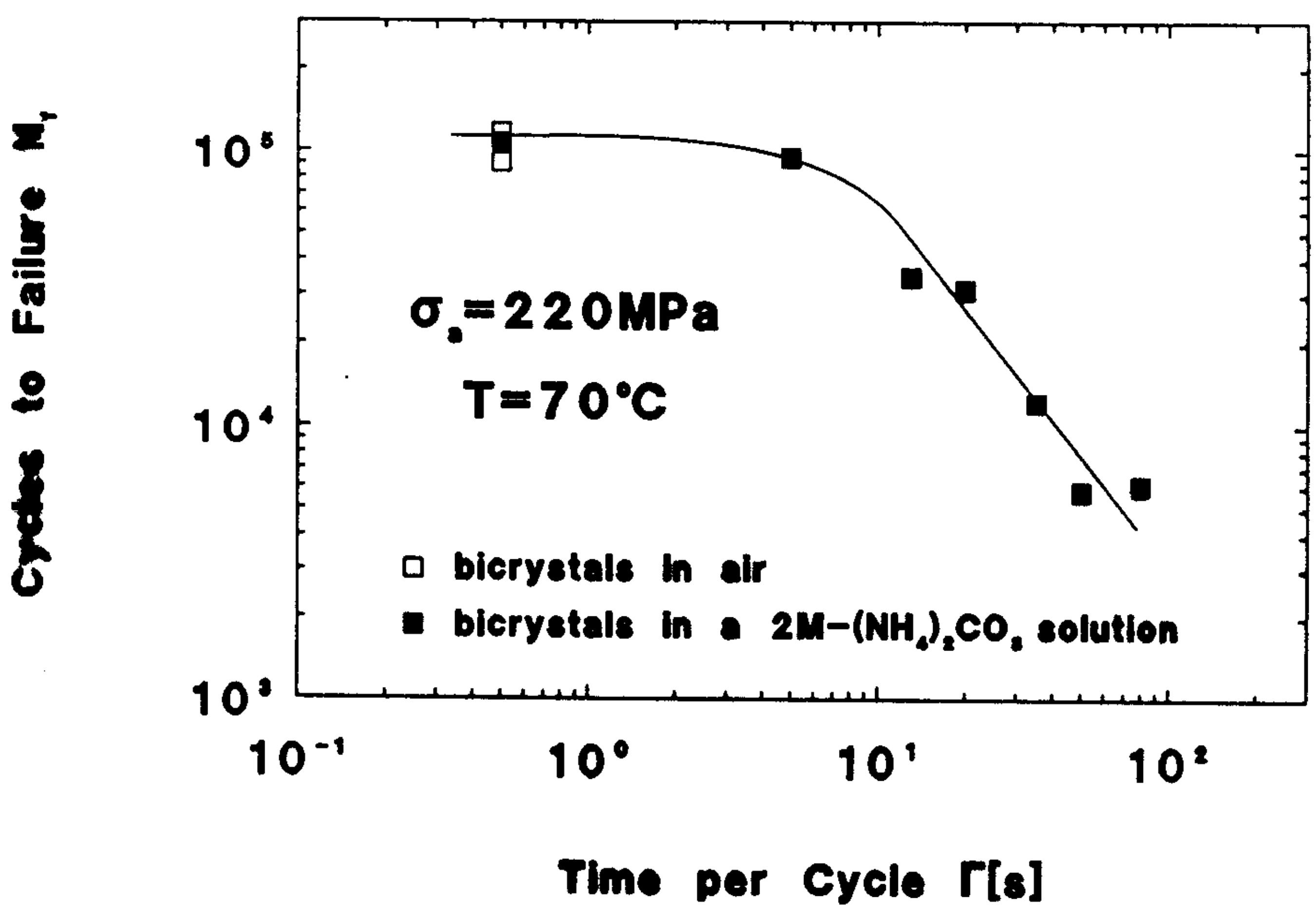
Cycles to Failure N_f
10^5
10^4
10^3
σ_a=220MPa
T=70°C
bicrystals in air
bicrystals in a 2M-$(NH_4)_2CO_3$ solution
10^{-1}
10^0
10^1
10^2
Time per Cycle Γ[s]

...[illegible] ... frequency ... [illegible]

failure for polycrystals and bicrystals.

For low frequencies poly- and bicrystals show the same reduction in life.

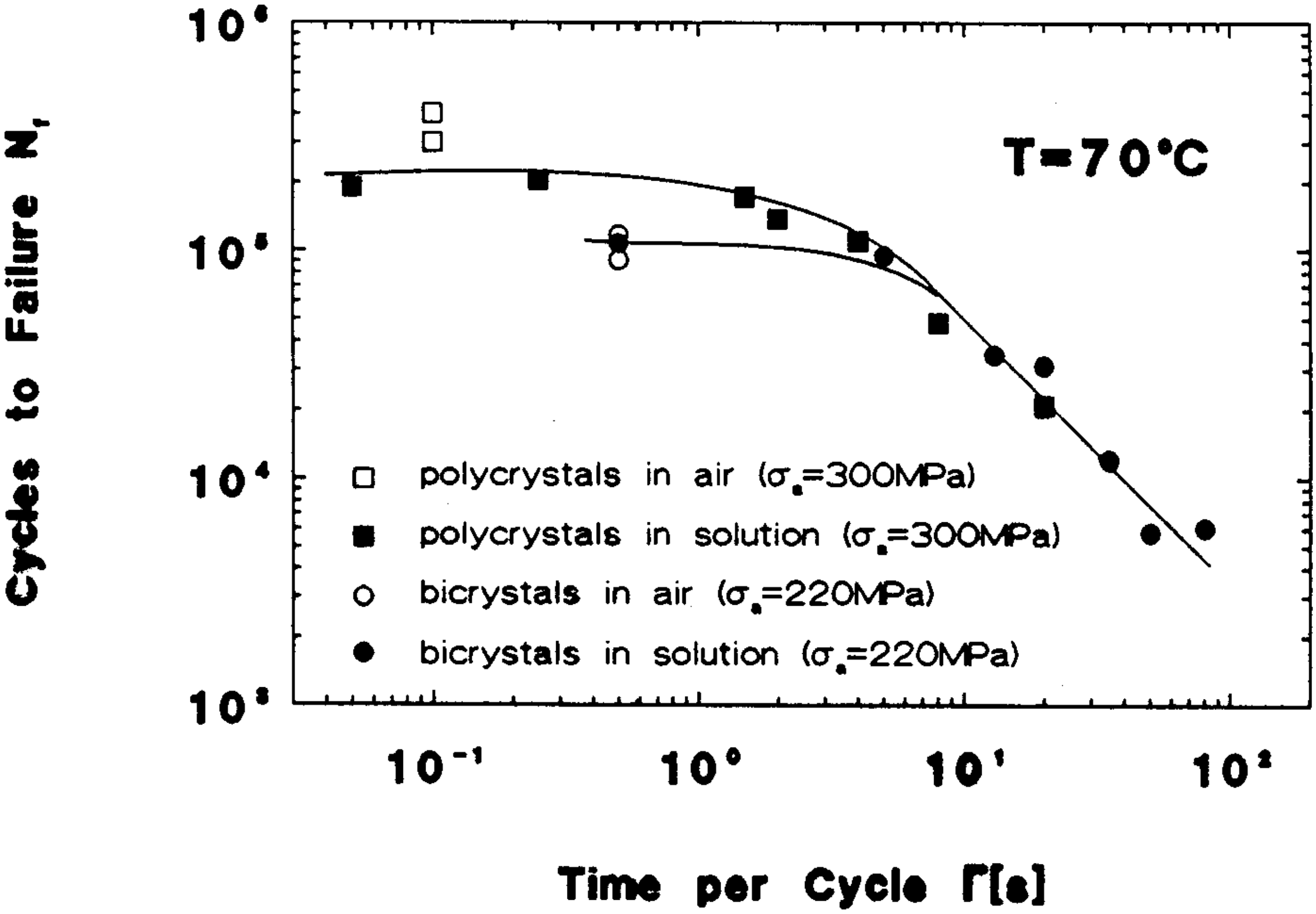

SUMMARY

Anodic Environments

Clean boundaries can be sensitive to SCC.
Segregation can enhance or inhibit SCC.
Crack growth rate strongly depends on the local slip distribution.
Special boundaries can reduce the crack nucleation stress by a factor of 2.
Corrosion Fatigue can reduce the fatigue life by orders of magnitude.
Reduction in life due to enhanced growth rate of micro cracks.

Cathodic Environments

Cracks do neither nucleate at nor propagate along clean boundaries.
After segregation of sulfur or low fugacity hydrogen incompatible grain boundaries were prone to crack nucleation.
In high fugacity hydrogen all boundaries are sensitive.

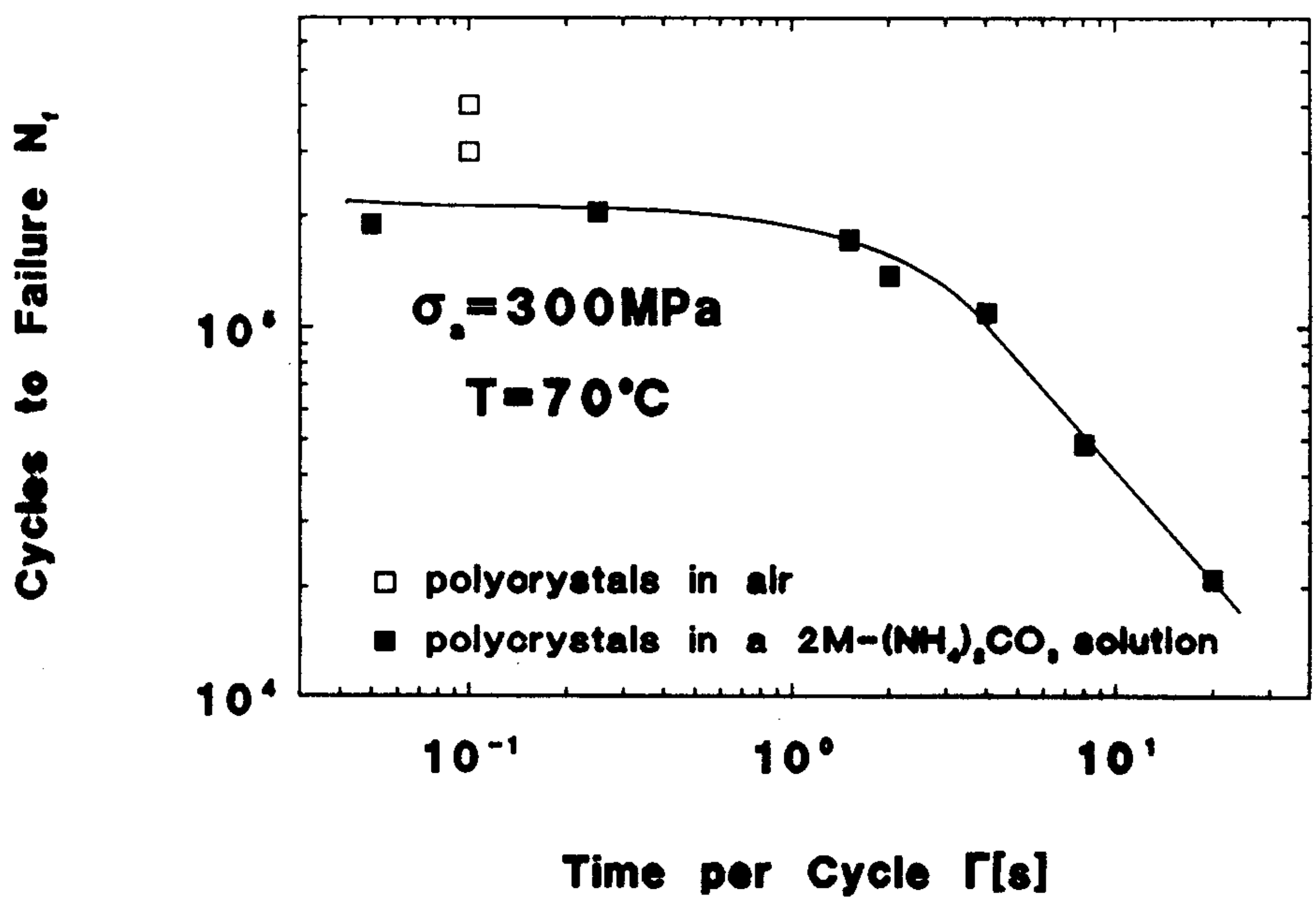

Cycles to Failure N_f
10^5
10^4
σ_a=300MPa
T=70°C
□ polycrystals in air
■ polycrystals in a 2M-$(NH_4)_2CO_3$ solution
10^{-1}
10^0
10^1
Time per Cycle Γ[s]

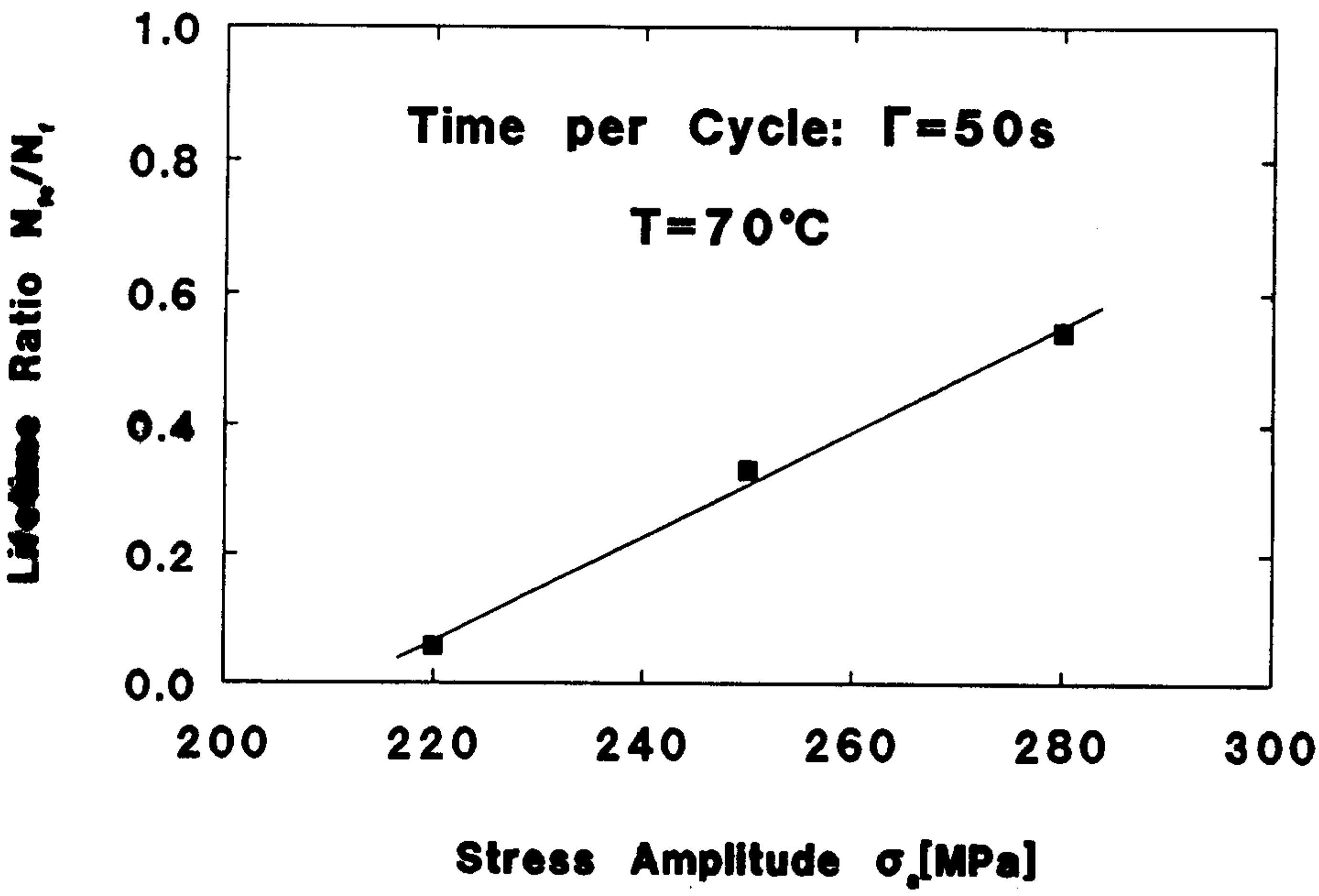

Time per Cycle: Γ=50s
T=70°C
1.0
0.8
0.6
0.4
0.2
0.0
Lifetime Ratio N/N
200
220
240
260
280
300
Stress Amplitude σ[MPa]

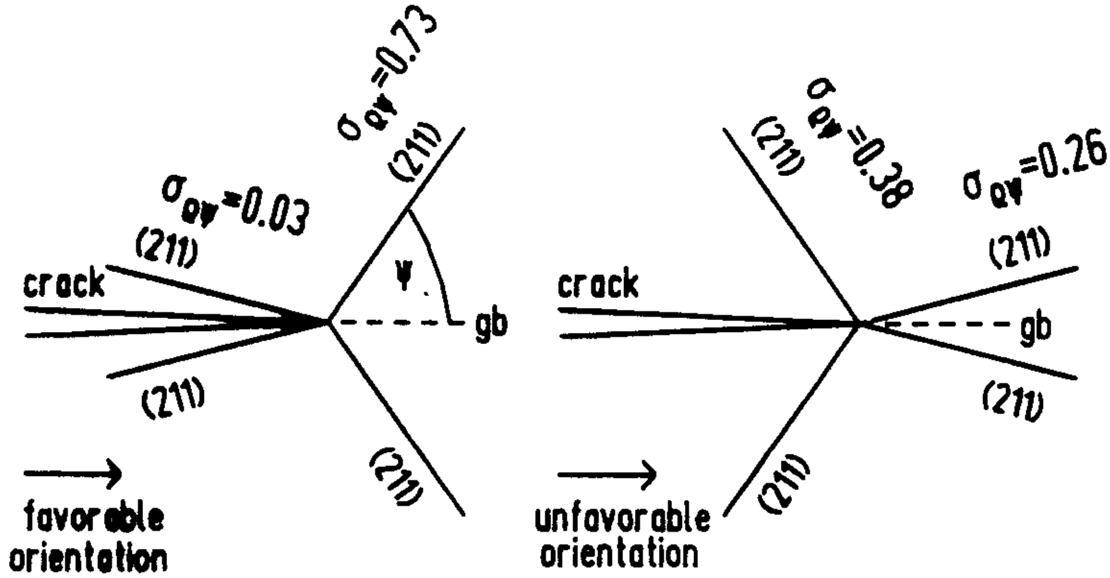

crack
σ_{eq}=0.03
(211)
(211)
σ_{eq}=0.73
(211)
ψ
gb
(211)
favorable orientation
crack
(211)
σ_{eq}=0.38
σ_{eq}=0.26
(211)
gb
(211)
(211)
unfavorable orientation

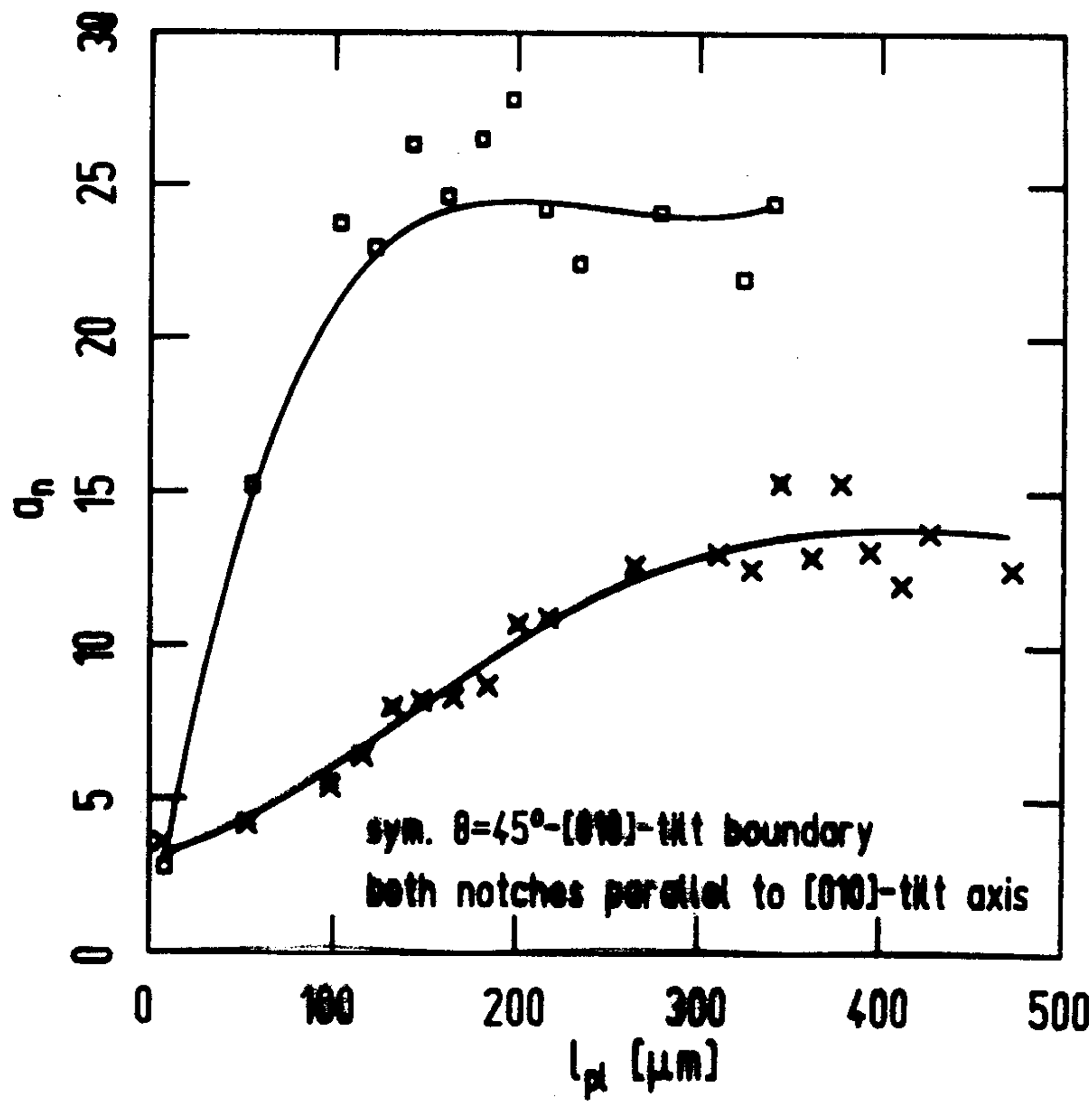

a_n
0
5
10
15
20
25
30
0
100
200
300
400
500
l_{pl} [μm]
sym. θ=45°-[010]-tilt boundary
both notches parallel to [010]-tilt axis

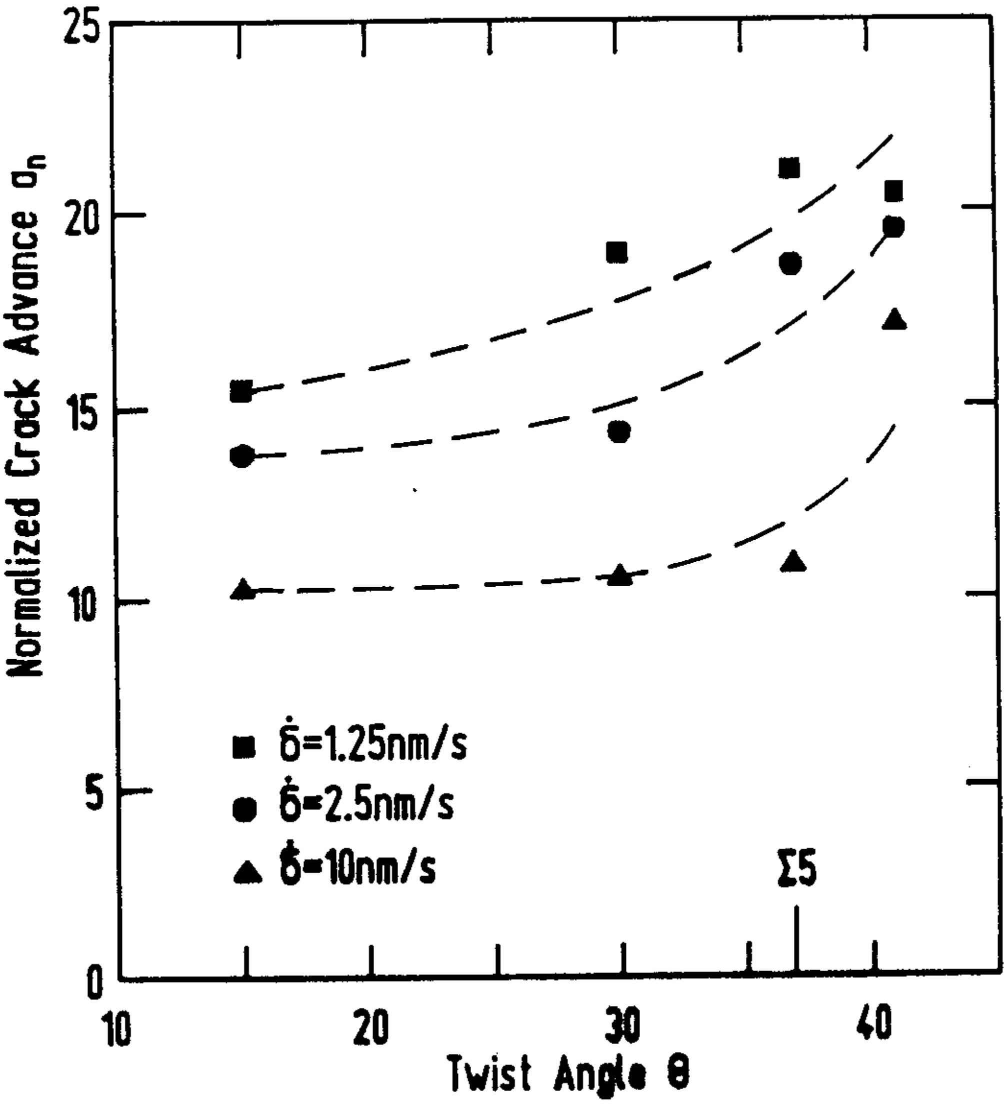

25
20
15
10
5
0
Normalized Crack Advance a_n
$\dot{\delta}$=1.25nm/s
$\dot{\delta}$=2.5nm/s
$\dot{\delta}$=10nm/s
Σ5
10
20
30
40
Twist Angle θ

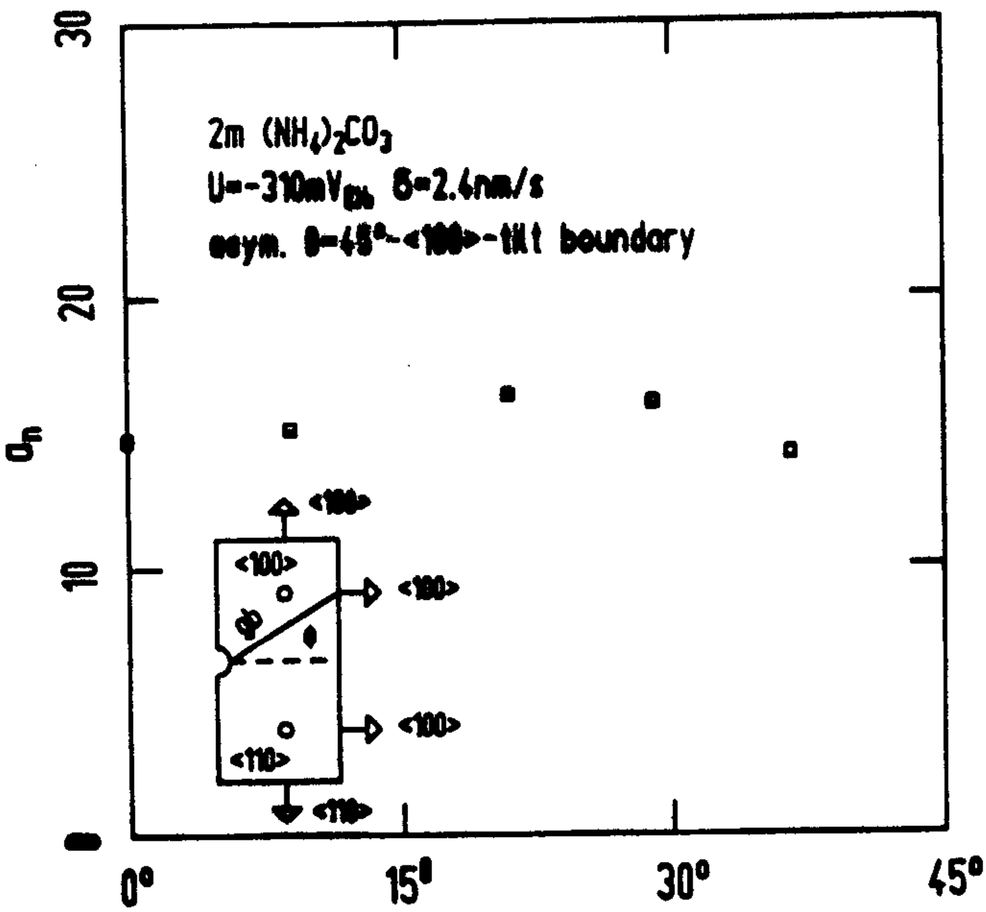

30
20
10
a_n
2m $(NH_4)_2CO_3$
U=-310mV, $\dot{\delta}$=2.4nm/s
<100>
<110>
0°
15°
30°
45°
angle of inclination ϕ

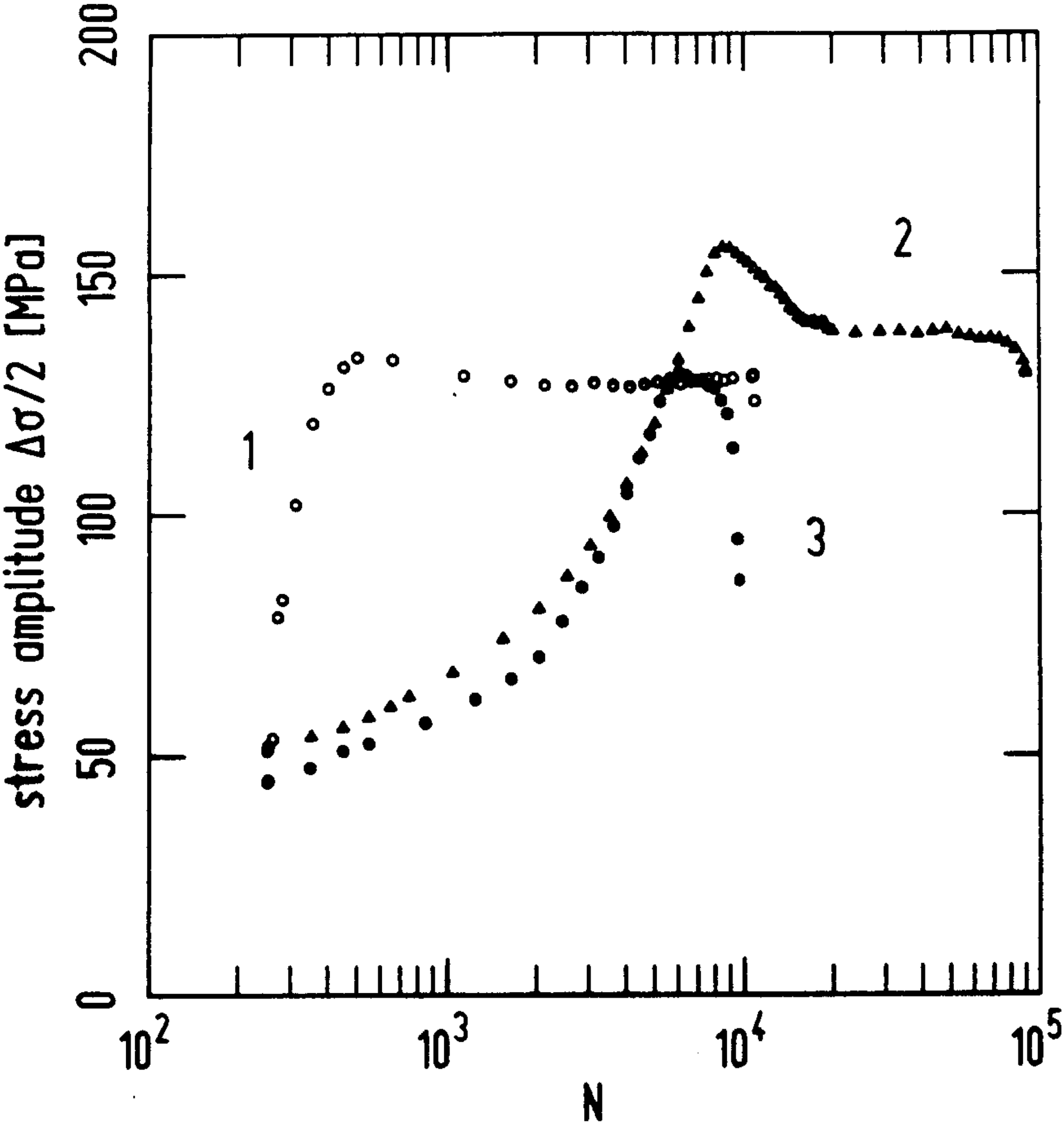

stress amplitude Δσ/2 [MPa]
0
50
100
150
200
10^2
10^3
10^4
10^5
N
1
2
3